Exp Physiol 98.7 (2013) pp 1164–1177

Research Paper

Resolution of hyposmotic stress in isolated mouse ventricular myocytes causes sealing of t-tubules

I. Moench, K. E. Meekhof, L. F. Cheng and A. N. Lopatin

Department of Molecular and Integrative Physiology, University of Michigan, Ann Arbor, MI, USA

New Findings

- **What is the central question of this study?**
  The t-tubules of ventricular myocytes are critical elements in excitation–contraction coupling. They become disorganized or even lost in various cardiac pathologies. However, the mechanisms leading to disruption of t-tubules are essentially unknown. This study was designed to identify physiologically relevant processes that underlie remodelling of t-tubules.
- **What is the main finding and its importance?**
  We show that the resolution of physiologically relevant hyposmotic swelling, not the application of osmotic shock itself, leads to dramatic t-tubular remodelling, including the sealing of individual t-tubules. The results point to an important and probably general mechanism of acute and fast stress-induced t-tubular remodelling that may underlie various relevant pathologies of the heart.

It has recently been shown that various stress-inducing manipulations in isolated ventricular myocytes may lead to significant remodelling of t-tubules. Osmotic stress is one of the most common complications in various experimental and clinical settings. This study was therefore designed to determine the effects of a physiologically relevant type of osmotic stress, hyposmotic challenge, to the integrity of the t-tubular system in mouse ventricular myocytes using the following two approaches: (1) electrophysiological measurements of membrane capacitance and inward rectifier (I_{K1}) tail currents originating from K^+ accumulation in t-tubules; and (2) confocal microscopy of fluorescent dextrans trapped in sealed t-tubules. Importantly, we found that removal of '0.6 Na' (60% NaCl) hyposmotic solution, but not its application to myocytes, led to a ∼27% reduction in membrane capacitance, a ∼2.5-fold reduction in the amplitude of the I_{K1} tail current and a ∼2-fold reduction in the so-called I_{K1} 'inactivation' (due to depletion of t-tubular K^+) at negative membrane potentials; all these data were consistent with significant detubulation. Confocal imaging experiments also demonstrated that extracellularly applied dextrans become trapped in sealed t-tubules only upon removal of hyposmotic solutions, i.e. during the shrinking phase, but not during the initial swelling period. In light of these data, relevant previous studies, including those on excitation–contraction coupling phenomena during hyposmotic stress, may need to be reinterpreted, and the experimental design of future experiments should take into account the novel findings.

(Received 8 February 2013; accepted after revision 11 April 2013; first published online 12 April 2013)
Corresponding author A. N. Lopatin: University of Michigan, Department of Molecular & Integrative Physiology, Room 7812, Medical Science II, 1150 West Medical Center Drive, Ann Arbor, MI 48109, USA. Email: alopatin@umich.edu

I. Moench and K. E. Meekhof contributed equally to this work.

DOI: 10.1113/expphysiol.2013.072470

Introduction

Osmotic stress is a common complication during various experimental and clinically relevant conditions. Numerous studies over more than half a century showed that both hyperosmotic and hyposmotic challenges to cardiac tissues and cells lead to a multitude of consequences, which are largely (although not exclusively) detrimental to their electrical and contractile properties. The most detailed and mechanistic studies have begun with the introduction of enzymatically isolated cardiac myocytes and use of the patch-clamp technique (for review see Vandenberg *et al.* 1996), targeting, in particular, the central phenomenon of excitation–contraction (EC) coupling. It has been shown that various types of osmotic shock lead to significant changes in many sarcolemmal currents, including Cl^- currents (Sorota, 1992; Vandenberg *et al.* 1994), delayed rectifier currents I_{Ks} and I_{Kr} (Rees *et al.* 1995), Ca^{2+} currents and currents generated by transporters (Whalley *et al.* 1991, 1993; for review see Cazorla *et al.* 1999). Osmotic regulation of Ca^{2+} currents has received the most attention, and studies have shown that the effects of osmotic stress are fairly complex and depend, in particular, on the type of cardiac cell (e.g. atrial *versus* ventricular). For example, it has been shown that during osmotically induced swelling, the L-type Ca^{2+} current increases in rabbit atrial cells (Matsuda *et al.* 1996) and decreases in rat ventricular myocytes (Brette *et al.* 2000), while swelling produces virtually no changes in guinea-pig ventricular myocytes (Groh *et al.* 1996). Detailed analysis of the time course of osmotic effects in rat and rabbit ventricular myocytes shows that the changes in the magnitude of the L-type Ca^{2+} current upon application of hyposmotic solution display biphasic behaviour, with an initial increase followed by downregulation at later times (Li *et al.* 2002; Luo *et al.* 2010). Similar biphasic phenomena were also observed for other relevant parameters, such as cell shortening (Li *et al.* 2002), action potential duration and loading of the sarcoplasmic reticulum (SR; Brette *et al.* 2000).

It is clear that the changes in membrane stretch and water content (leading to dilution or concentration of intracellular milieu) in cardiac myocytes upon osmotic stress are the initial general events, which lead to a multitude of complicated but specific consequences for distinct ion channels, transporters, intracellular organelles (e.g. SR) and integrative parameters, such as action potential and EC coupling. In ventricular myocytes, however, there is another general feature of paramount importance for the overall activity of the myocyte that may directly underlie and explain numerous osmotic phenomena, namely the t-tubules. It has long been known that t-tubules in skeletal muscle can be removed (sealed) by strong hyperosmotic shock with glycerol (Eisenberg & Eisenberg, 1968; Howell, 1969) or formamide (Argiro, 1981), with detubulation occurring upon withdrawal of the osmolite.

The 'formamide version' of the detubulation method, which uses a very high concentration of formamide (1.5 M), was introduced in the cardiac field by Kawai *et al.* (1999) and provided an excellent experimental tool for numerous t-tubular studies. However, the potential role of shock-induced detubulation in physiologically and pathophysiologically relevant conditions is essentially unknown. To our knowledge, the only study where an attempt was made to look into the state of t-tubules during hyposmotic stress was that by Brette *et al.* (2000). The results were negative; swelling of rat ventricular myocytes in hyposmotic solution did not lead to detubulation. Importantly, however, the integrity of t-tubules in the study by Brette *et al.* (2000) was assessed only during the swelling phase (i.e. application of hyposmotic solution).

In this study, we demonstrate that despite previous unsuccessful attempts to elucidate the effects of physiologically relevant osmotic challenges on t-tubules, their remodelling does occur. Specifically, we describe a novel and unexpected phenomenon of strong t-tubular remodelling, which occurs almost exclusively upon resolution (shrinking phase) but not during hypotonic stress itself (swelling phase). Experiments with isolated mouse ventricular myocytes show that washout of commonly used hypotonic solutions with osmolarity only ~25% less than normal leads to significant-to-dramatic t-tubular remodelling, comparable to detubulation produced by 1.5 M formamide. Given that nearly all hypotonic challenges are eventually resolved, the potential physiological significance of this phenomenon is clear and will need to be addressed accordingly. The data also show that many relevant previous studies may need to be reinterpreted, and the experimental design of future experiments should take into account the novel findings.

Methods

Animals

All experiments involving mice were carried out in accordance with the *Guide for the Care and Use of Laboratory Animals* (8th edition; Committee for the Update of the Guide for the Care and Use of Laboratory Animals, National Research Council; The National Academic Press, Washington, DC, USA) and protocols approved by the veterinary staff of the University Committee on Use and Care of Animals at the University of Michigan.

Solutions

Osmolarity was measured using Vapro Osmometer 5520 (Wescor, ELITechGroup, France) and values of osmolarity are presented as means ± SD.

Tyrode solution (Tyr; modified) had the following composition (mM): 137 NaCl, 5.4 KCl, 0.5 $MgCl_2$, 0.3 $CaCl_2$, 0.16 NaH_2PO_4, 3 $NaHCO_3$, 5 Hepes, 5.5 glucose; pH adjusted to 7.35 with NaOH; osmolarity 278.7 ± 3.5 mosmol l^{-1}. 10 mM glucose was used in patch-clamp experiments.

Solutions for isolation of ventricular myocytes (filtered using 0.22 μm filter) (mM). Solution A had the following composition (mM): 122 NaCl, 5.4 KCl, 4 $MgCl_2$, 0.16 NaH_2PO_4, 3 $NaHCO_3$, 15 Hepes, 10 glucose, 0.1 μM EGTA; pH adjusted to 7.35 with NaOH; 279.7 ± 6.4 mosmol l^{-1}. Solution B comprised 50 ml solution A + 30 mg collagenase (Type 2; Worthington Biochemical Corporation, Lakewood, NJ, USA). Solution C comprised 180 ml solution A + 900 mg bovine serum albumin + 250 mg taurine; 288.7 ± 3.5 mosmol l^{-1}.

Pipette solution KINT comprised (mM): 140 KCl, 0.5 EGTA, 10 Hepes, 5 K_2ATP; pH adjusted to 7.3 with KOH; 280.7 ± 2.3 mosmol l^{-1}. 0.2 $CaCl_2$/2 EGTA was used in experiments in Fig. 7.

Standard phosphate buffer solution (PBS) had an osmolarity of 267.2 ± 2.5 mosmol l^{-1}; PBS_40 (PBS diluted by 40% with H_2O) had an osmolarity of 193.3 ± 2.9 mosmol l^{-1}; and 10% PBS in Tyr solution had an osmolarity of 277.8 ± 1.3 mosmol l^{-1}.

Osmotically modified solutions. The 0.6 Na solution consisted of Tyr containing 60% NaCl (82.2 mM); 204.7 ± 4.2 mosmol l^{-1}. The 9% PBS_40 in 0.6 Na solution had an osmolarity of 201.0 ± 2.7 mosmol l^{-1}. The 0.8 Na solution consisted of Tyr containing 80% NaCl (109.6 mM); 241.5 ± 3.7 mosmol l^{-1}. The 0.6 Na/100 S solution consisted of 0.6 Na containing 100 mM sucrose; 284.9 ± 3.9 mosmol l^{-1}. The 0.6 Na/200 S solution consisted of 0.6 Na containing 200 mM sucrose; 372.6 ± 3.0 mosmol l^{-1}.

Most experiments were performed using 0.6 Na solution where both NaCl concentration and osmolarity are changed. Stronger effects induced by this solution allow for easier quantification of the data as well as for revealing the modulating effect of NaCl in experiments involving 0.6 Na/100 S where only osmolarity is modified.

Five milligrams of voltage-sensitive dye di-8-ANEPPS (Life Technologies, Carlsbad, CA, USA) was dissolved in 1 ml of DMSO and used as a stock (stored at 4°C). Working solution was prepared as 50:50 v/v mix of di-8-ANEPPS stock and 20% pluronic acid (to facilitate the solubilization of di-8-ANEPPS).

Isolation of mouse ventricular cardiomyocytes

Ventricular myocytes were isolated from the hearts of adult (∼2- to 6-month-old) C57BL/6 mice of either sex anaesthetized with Avertin (20 μl g^{-1} of working solution; I.P.) using collagenase treatment. The Avertin stock solution was prepared as follows (McLerie & Lopatin, 2003): 10 g of tribromoethanol alcohol (Sigma-Aldrich, St. Louis, MO, USA) was mixed with 10 ml of *tert*-amyl alcohol (Aldrich, USA) and stored at −20°C. The working solution of ∼2.5% was prepared by mixing of 1 ml of Avertin stock with 39 ml of PBS and the addition of 1 mg ml^{-1} of heparin (Sigma, St Louis, MO, USA; 187 USP unit/mg). Briefly, hearts were perfused retrogradely (Langendorff perfusion) through the aorta with appropriate solutions at a constant pressure of ∼115 cmH_2O and temperature of ∼28°C using a water-jacketed supply tube. Atria were removed and the atrioventricular valve was surgically destroyed. Solution A was applied for ∼5 min, followed by solution B. Approximately ∼2 min later 44 μM Ca^{2+} was added, and the heart was digested with solution recirculation for another 33 min. The lower part of the heart (approximately three-quarters) was cut off and the right ventricle outer wall removed. The left ventricle was opened, sliced into about six to eight pieces, the tissue transferred to a 15 ml tube containing 10 ml of solution B and triturated at ∼28°C on a rocker for ∼15 min. The myocyte suspension was filtered and procedure repeated with tissue chunks up to five times with an increasing proportion of solution C. The myocytes were usually optimally isolated at steps 4–5. Myocytes were stored in respective solutions at room temperature (RT; 20–23°C) and used in experiments within 1–5 h postisolation.

Patch-clamp measurements

Ionic currents were recorded in the whole-cell configuration of patch-clamp technique (Hamill *et al.* 1981) at RT essentially as described by Cheng *et al.* (2011), with a few minor modifications. In particular, the resistance of the patch pipettes (KIMBLE glass; no. 73813) varied from 2 to 4 MΩ when filled with KINT solution. In few experiments, pipette tips were coated with a mixture of mineral oil and paraffin with the intention of reducing stray capacitance of the pipette. Series resistance was always compensated, leading to 2–3 MΩ access resistance. The data were filtered at 2 kHz. During patch-clamp measurements, the myocytes were continuously superfused with appropriate solutions using a flow chamber allowing for changes of solutions within a few seconds. A 3 M KCl–agar salt bridge for earthing the bath is (always) used in order to minimize potential voltage offsets in experiments involving changes of extracellular solutions.

Membrane capacitance (C_M) was measured using the Clampex (Molecular Devices, Sunnyvale, CA, USA) built-in algorithm employing mono-exponential fit to capacitative current in response to a $\Delta V_M = 5$ mV depolarizing voltage step from a holding potential of −75 mV.

The $I_{K,end}$ and inward rectifier tail currents ($I_{K1,tail}$) and I_{K1} 'inactivation' (Fig. 6*A* and *C*) were analysed as described by Cheng *et al.* (2011). Briefly, ionic currents were recorded in response to a 400 ms voltage step to +50 mV followed by repolarization back to a holding potential of −75 mV. The $I_{K,end}$ is the current at the end of depolarizing step. The $I_{K1,tail}$ current was fitted using a two-exponential function, as follows: $A_1 e(-\frac{t}{\tau_1}) + A_2 e(-\frac{t}{\tau_2}) + C$, where A_1 and A_2 are the amplitudes and τ_1 and τ_2 are the corresponding time constants of exponential components, t is the time and C is the steady state current. Approximately ∼7 ms of the current traces was excluded from the fit to avoid a contribution from capacitative currents, and the amplitudes of individual exponential components (A_1 and A_2) were then recalculated to 0 time using measured time constants. Finally, the ratio $I^N_{K1,tail} = |\frac{(A_1+A_2)}{I_{K,end}}|$ was calculated.

The I_{K1} was measured in response to a 400 ms voltage step from a holding potential of −75 to −120 mV. The time course of I_{K1} 'inactivation' ($I_{K1,inact}$) was fitted with a two-exponential function and normalized current calculated as $I^N_{K1,inact} = \frac{(A_1+A_2)}{I_{K1(-120)}}$, where A_1 and A_2 are the amplitudes of the time-dependent component of I_{K1} 'inactivation' and $I_{K1(-120)}$ is the (peak) magnitude of I_{K1} recalculated (Δt ∼8 ms) to time 0.

Formamide-induced detubulation of cardiac myocytes

Formamide-induced osmotic shock was implemented essentially as described by Kawai *et al.* (1999) except that solution C was used for detubulation steps (i.e. washout of formamide).

Osmotic shocks in dextran trapping experiments

High concentration of fluorescent dextran must be used in order to visualize and quantify rather small sealed t-tubules. Therefore, the following procedures were used. 3,000 MW (3K) tetramethylrhodamine (red) anionic dextran (Invitrogen, USA) was dissolved in PBS at concentration 10 mg ml^{-1}, part of the solution diluted by 40% with H_2O (PBS_40; to better preserve the osmolarity of 0.6 Na solution when adding dextran) and both solutions stored at −20°C for future use.

'Late' application of dextran (see Fig. 2*A2*). A small aliquot (up to few hundred microlitres) of enzymatically digested myocytes was diluted in a large volume (usually 10 ml) of desired solution (e.g. 0.6 Na for hyposmotic swelling) and the timer started. Myocytes were concentrated by centrifugation (2 minutes at 48 *g*; all other centrifugations were performed using same parameters), then 10 μl of cell suspension was transferred into separate tube and 1 μl of dextran stock (in PBS or PBS_40) added ∼2 min before removal of the hyposmotic solution to allow dextran to fill accessible t-tubules. Normal (near isotonic) solution consisting of 90 μl of Tyr and 10 μl 3K dextran stock (in PBS) was added at 7 min in order to initiate myocyte shrinkage. Addition of dextran dissolved in appropriate solution (PBS or PBS_40) does not lead to any significant changes in osmolarity of the test solution. In order to remove most of the extracellular dextran, cells were resuspended in ∼10 ml of Tyr 5 min after the osmotic shock, concentrated by centrifugation to <∼100 μl and resuspended again in ∼0.5–1 ml of solution C.

'Early' application of dextran (Fig. 2*A1*). One microlitre of dextran stock was added to 10 μl of cell suspension immediately before osmotic shock. Hyposmotic solution consisted of 300 μl 0.6 Na and 30 μl of dextran stock. Approximately 2 min before removal of the hyposmotic solution, myocytes were resuspended in 10 ml of dextran-free 0.6 Na solution (in order to dilute dextran ∼30-fold) and concentrated by centrifugation. Exactly 7 min after the application of hyposmotic solution, cells were resuspended in ∼10 ml of normal Tyr in order to initiate cell shrinkage. Finally, myocytes were concentrated by centrifugation and resuspended again in ∼0.5–1 ml of solution C.

In experiments using low-NaCl (e.g. 0.6 Na/100 S) solution as the initial control instead of normal Tyrode solution, myocytes were pre-incubated in that solution for 5 min before application of the test solution.

All experiments were performed along with appropriate controls including all steps (dye mixing, centrifugations etc.) but using normal Tyrode solution instead of osmotically modified solutions.

Confocal imaging and image analysis

Confocal imaging was performed using an Olympus FV-500 microscope at the Microscopy and Image Analysis Laboratory (University of Michigan, Ann Arbor, MI, USA) using a ×60 oil immersion objective. Confocal images were visualized and analysed using ImageJ software (http://imagej.nih.gov). In experiments using membrane labelling, myocytes were exposed postshock (i.e. after washout of test solutions) to di-8-ANEPPS (∼0.5 μl working solution in 300 μl of cell suspension) for ∼10–30 min at room temperature. In all experiments, only fluorescence originating from within the outline of

myocytes was analysed. This was achieved by manually creating a region of interest contained within the border (but not including it) of the myocyte and then calculating mean 'intracellular' fluorescence. This procedure eliminates any contribution of fluorescence from traces of extracellular dextran remaining after the washout procedure and di-8-ANEPPS fluorescence originating from the outer sarcolemma (including highly convoluted intercalated discs). The data were corrected for background fluorescence measured in myocytes processed in an identical manner to that in test experiments but without application of osmotic shock (i.e. including the presence of 3K dextran and centrifugations at specific steps). Given that we are concerned with only the total amount of fluorescence of trapped dextran (proportional to the volume of sealed t-tubules) and total amount of 'intracellular' fluorescence of di-8-ANEPPS (proportional to the surface area of accessible t-tubules) neither image deconvolution nor other sophisticated approaches (e.g. super-resolution microscopy techniques) useful for resolving the fine structure of t-tubules were necessary. We found that the use of 'red' dextran is superior to the 'green' version of the compound because of significantly lower background fluorescence of myocytes in the red part (*versus* green) of the spectra.

Statistics

Data are presented as means ± SEM except for the data on osmolarity (in the preceeding subsections), for which means ± SD are used. All data used in image analysis were corrected for the background fluorescence. Statistical significance was calculated using Student's two-tailed *t* test with the exception of the data in Fig. 7, for which Student's paired *t* test was used. Throughout the manuscript asterisks *, ** and *** represent $P < 0.05$, <0.01 and <0.001, respectively. All data, with the exception of largely introductory and confirmatory data in Fig. 1, are from at least two heart preparations, with multiple myocytes (9–50; exact numbers indicated in the text) used in each experimental setting.

Results

Effects of hyposmotic stress on the dimensions of the cells

Figure 1*A* shows a representative example of an experiment in which a myocyte was first superfused in a flow chamber with Tyrode solution (Tyr), in order to wash out storage solution (C), then hyposmotic solution 0.6 Na applied and myocytes then returned back to Tyr solution. The dimensions of the myocytes stabilized within ∼3–4 min in hyposmotic solution and returned back to normal also within ∼3–4 min upon resolution of stress. The speed of the change of solutions in the chamber, more specifically the speed of change around the individual cells, is likely to be one of the contributing factors to the kinetics of the swelling, which potentially may occur faster with faster speeds of perfusion (this was not investigated further). For practical purposes, however, in order to be sure that the swelling of myocytes in 0.6 Na and 0.8 Na reached the steady state, 7 min exposure was used (rather than 15 min exposure to formamide as in the study by Kawai *et al.* 1999). Consistent with the previous studies, the myocytes responded to hyposmotic challenge primarily by changes in the cell width rather than length (Roos, 1986; Boyett *et al.* 1991; Brette *et al.* 2000; Fig. 1*B*). The change in width of the myocytes was nearly fivefold larger than the change in their length, i.e. 13.3 ± 1.2 and 2.7 ± 0.5% ($n = 10$; $P < 0.001$) relative to initial values for width and length, respectively. Myocyte dimensions returned back to normal within ∼1% precision upon resolution of stress. In contrast to some studies (Brette *et al.* 2000), application of hyposmotic solutions was not accompanied by any visual deterioration of myocytes, such as membrane blebbing.

Resolution of hyposmotic stress, but not the stress itself, leads to sealing of t-tubules

Figure 2 summarizes the central finding of this study. The effects of hyposmotic stress on the integrity of the t-tubular system were assessed using fluorescent dextrans (Brette *et al.* 2002). Ventricular myocytes were first exposed to 0.6 Na solution, as indicated in Fig. 2*A*, with extracellular 3K red dextran present during different phases of the stress (protocols 1 and 2; Fig. 2*A*), and confocal images taken within ∼2 h postshock in normal Tyrode solution to assess the presence of dextran (present only for ∼5 min after the

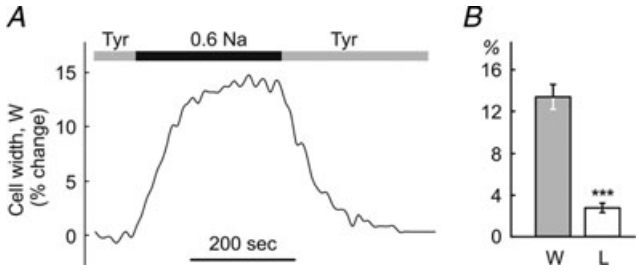

Figure 1. Effects of hyposmotic challenge on dimensions of ventricular myocytes
A, application of 0.6 Na hyposmotic solution to ventricular myocytes leads to fast and significant changes in their width. Dimensions of myocytes return to normal upon reapplication of control Tyrode solution (Tyr). *B*, the changes in the width (W) of the myocytes are approximately fivefold larger than changes in their length (L). The change in dimensions is expressed as a percentage relative to the resting values in Tyr solution.

resolution of shock) potentially trapped in sealed or highly constricted t-tubules. If extracellular dextran was present before and during the swelling phase caused by application of 0.6 Na solution, but not at or during cell shrinkage (Fig. 2*A*), confocal imaging of myocytes after the recovery from shock did not reveal any significant intracellular fluorescence (Fig. 2*Ba*). However, when dextran was present in the 0.6 Na solution immediately before and during shrinkage phase (Fig. 2*A*, protocol 2) significant 'intracellular' fluorescence could then be observed easily (Fig. 2*Bb*). The only plausible explanation for the results is that dextran was trapped in sealed t-tubules at the time of or shortly after the washout of 0.6 Na solution. The magnitude of 'intracellular' fluorescence of dextran observed in the whole cell is seemingly quite small (Fig. 2*Bbi*), as it may be perceived by looking at the images. However, it should be taken into account that t-tubules are relatively sparse and thin (in large degree, they are point-type objects) and their volume relative to that that of the whole cell is also quite small, less than few per cent (Stewart & Page, 1978; Soeller & Cannell, 1999). In fact, in contrast to this potential illusion, some pixels in the images are saturated due to intense fluorescence of dextran trapped in sealed t-tubules. Zooming into the image (Fig. 2*Bbii*) or increasing its contrast (Fig. 2*Bbiii*) highlights the effect. Specifically, the density of 3K dextran fluorescence (the amount of fluorescence per unit area within the myocyte borders; arbitrary units but identical imaging conditions; see Methods for details) was as follows: intracellular background fluorescence (control), 4.0 ± 0.1; 'early' application of 3K dextran as in protocol 1 (Fig. 2*A*), 3.9 ± 0.1; and 'late' application of dextran as in protocol 2 (Fig. 2*A*), 6.0 ± 0.5 ($n = 24$, 24 and 24 for these conditions, respectively; $P < 0.001$). For presentation purposes in Fig. 2*C*, the data were first corrected for background fluorescence by subtracting fluorescence measured in control myocytes, which were treated identically to test myocytes (i.e. including all steps such as centrifugations) in the presence of extracellular dextran but using isosmotic solutions instead of 0.6 Na hyposmotic solution. The data were further normalized to those in protocol 2 (Fig. 2*A*). Importantly, the quantification procedure for the fluorescence (see Methods) is robust, because it does not require any detailed knowledge of the fine structure of t-tubules (which is of no concern in this study), and the data show dramatic effects of the removal of hyposmotic shock on the amount of trapped dextran, suggesting significant t-tubular remodelling (sealing of t-tubules).

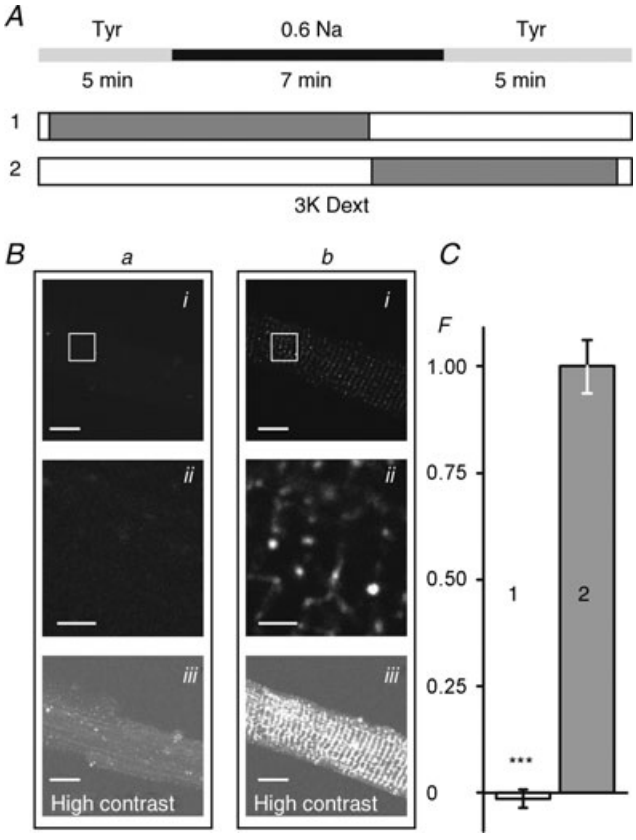

Figure 2. Sealing of t-tubules occurs exclusively during resolution of hyposmotic shock
A, timing (±30 s) of the application of 0.6 Na hyposmotic solution and 3K red fluorescent dextran (protocols 1 and 2). *B*, myocytes were imaged in dextran-free solution using a confocal microscope (with identical settings) within 1–2 h after hyposmotic shock. *Bai* and *Bbi* images correspond to protocols 1 and 2, respectively. *Baii* and *Bbii* images are magnified replicas of the corresponding rectangular areas in *Bai* and *Bbi*. *Baiii* and *Bbiii* images are contrast-adjusted replicas of the *Bai* and *Bbi* images highlighting the overall magnitude of t-tubular sealing. *C*, the average intensity of intracellular fluorescence from within the outline of the myocytes (i.e. not including out-of-cell area; see Methods) was background corrected using the average intracellular fluorescence in cells that had undergone the complete protocol 2, but in the presence of Tyr solution instead of 0.6 Na solution. *F* is the relative fluorescence. The mean fluorescence in protocol 2 was set to 1. Bars in *B* represent 10 μm for *i* and *iii* and 2 μm for *ii*. Note that the small negative fluorescence in *C* reflects experimental error due to background correction.

The extent of hyposmotic t-tubular sealing

At this juncture, however, the above data do not provide enough information on the extent of hyposmotic detubulation relative, in particular, to that produced by formamide treatment (Kawai *et al.* 1999). The data in Fig. 3 compare the effects of formamide and various hyposmotic treatments on changes in the volume of sealed t-tubules. First, Fig. 3*B* shows that the relative amount of 3K dextran trapped in t-tubules is reduced from 1.00 ± 0.09 during treatment with 1.5 M formamide to about 0.51 ± 0.05, or by 50%, after application of 0.6 Na solution ($n = 26$, 27 and 27 for control, 0.6 Na and formamide conditions,

respectively; $P < 0.001$). This is a remarkable level of detubulation considering the relatively small change in osmolarity in 0.6 Na solution (~80 mosmol reduction relative to normal Tyr solution) compared with that in solution containing 1.5 M formamide (membrane-permeable agent; estimated osmolarity >1400 mosmol; A.N. Lopatin, unpublished observation). The data in Fig. 3*C* also show that hyposmotic detubulation, as one may expect, is a graded process with intermediate (but nevertheless significant) levels of 3K dextran trapping observed in less hyposmotic solutions, such as 0.8 Na. Specifically, after treatment with 0.8 Na solution the trapping of 3K dextran is reduced to 0.24 ± 0.03, or to ~25%, relative to 1.00 ± 0.04 after exposure to 0.6 Na solution ($n = 41$, 50 and 47 for control, 0.6 Na and 0.8 Na conditions, respectively; $P < 0.001$).

Figure 4 shows the effects of hyposmotic detubulation employing a more 'classical' approach for assessing detubulation using membrane-specific dye (Kawai *et al.* 1999; Cheng *et al.* 2011). Ventricular myocytes were shocked with 0.6 Na hyposmotic and 1.5 M formamide hyperosmotic solutions as described earlier (see Fig. 2 and Fig. 3 along with corresponding text) and the accessible sarcolemmal membrane was labelled with di-8-ANEPPS dye. Both types of treatments led to significant reduction of t-tubular labelling compared with that in control myocytes, indicating strong, yet quantitatively different, detubulation. Specifically, after the treatment with 0.6 Na solution, t-tubular fluorescence of di-8-ANEPPS was reduced to $43 \pm 2.4\%$ of that observed in control myocytes (or, alternatively, ~57% of the t-tubular membrane compartment was inaccessible). Consistent with the data in Fig. 3*B*, detubulation by formamide was more effective, with t-tubular labelling reduced to $24 \pm 1.5\%$ of that in control myocytes (or ~76% detubulation). With regard to quantitative comparisons of experiments employing membrane-specific and water-soluble dyes, it is important to mention the principal difference between the use of dextran and di-8ANEPPS, which is that the former reports the volume of sealed t-tubules while the latter reports the surface area of accessible membrane.

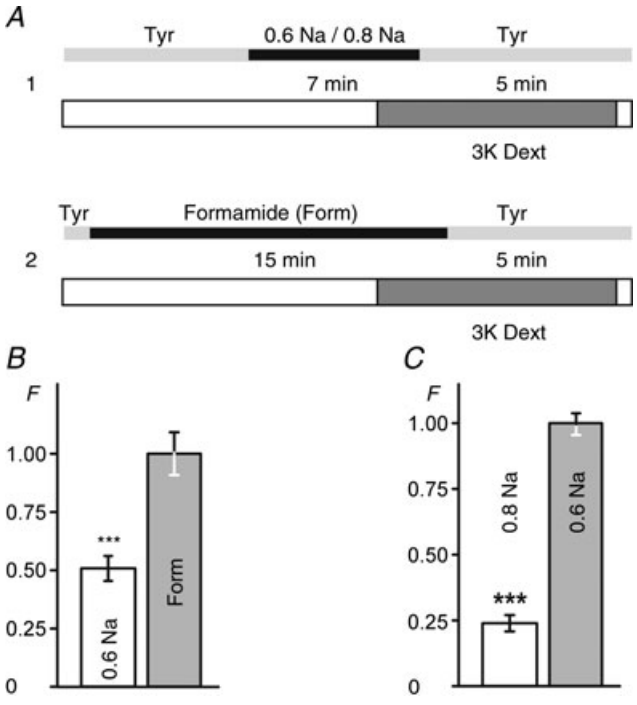

Figure 3. The extent of hyposmotic t-tubular sealing
A, timing of the application of various hyposmotic (protocol 1) and hyperosmotic formamide (Form)-containing solutions (protocol 2) using 'late' application of 3K fluorescent dextran (3K Dext; see Methods). *B*, the relative amount of trapped 3K dextran after stress with 0.6 Na solution is ~50% of that observed after formamide treatment. *C*, the relative amount of trapped 3K dextran after stress with 0.8 Na solution is ~25% of that of after treatment with 0.6 Na solution. *F* is the relative fluorescence. Mean fluorescence in *B* for formamide treatment and in *C* for treatment with 0.6 Na solution was set to 1.

The effects of NaCl, osmolarity and cell shrinkage on t-tubular sealing

It seemed reasonable to suggest that the effects of hyposmotic shock with 0.6 Na solution may, in fact, be due to changes in the concentration of NaCl rather than

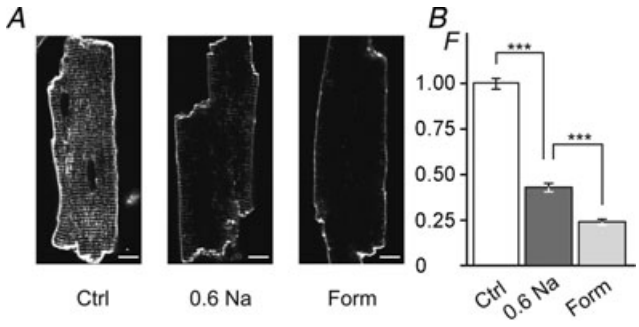

Figure 4. The effect of hypo- and hyperosmotic detubulation observed with the membrane-specific dye di-8-ANEPPS
A, ventricular myocytes were exposed to 0.6 Na hyposmotic or 1.5 M formamide hyperosmotic solutions for 7 and 15 min, respectively, returned to normal Tyr solution, labelled with di-8-ANEPPS dye along with control cells (Ctrl; not subjected to osmotic stress) and imaged using confocal microscopy. The Ctrl myocytes display strong intracellular fluorescence originating from t-tubular membranes. In contrast, both types of osmotic shock lead to significant reduction of 'intracellular' labelling consistent with detubulation. Scale bars represent 10 μm. *B*, quantification of 'intracellular' fluorescence (not including the outer sarcolemma or intercalated discs; see Methods). The amount of t-tubular fluorescence is reduced to ~43 and ~24% of that in control myocytes after treatment with 0.6 Na and 1.5 M formamide solutions, respectively. *F* is the relative fluorescence. Mean fluorescence for Ctrl was set to 1.

changes in osmolarity. Specifically, washout of 0.6 Na solution (the period of time when detubulation occurs) is associated with the return to both normal NaCl and normal osmolarity (Fig. 5*A*; protocol 0). Therefore, we first performed experiments in which osmolarity was kept normal throughout the procedure using 100 mM sucrose in 0.6 Na solution (0.6 Na/100 S solution) and therefore the concentration of NaCl was the only variable (Fig. 5*A*; protocol 1). No measurable trapping of 3K dextran was observed (Fig. 5*B*); -0.049 ± 0.001 compared with that in protocol 0, 1.00 ± 0.01 ($n = 20$, 20 and 20 for background control, protocol 0 and protocol 1, respectively; $P < 0.001$). The data strongly suggest that the change in osmolarity is the primary reason for detubulation upon treatment with hyposmotic 0.6 Na solution.

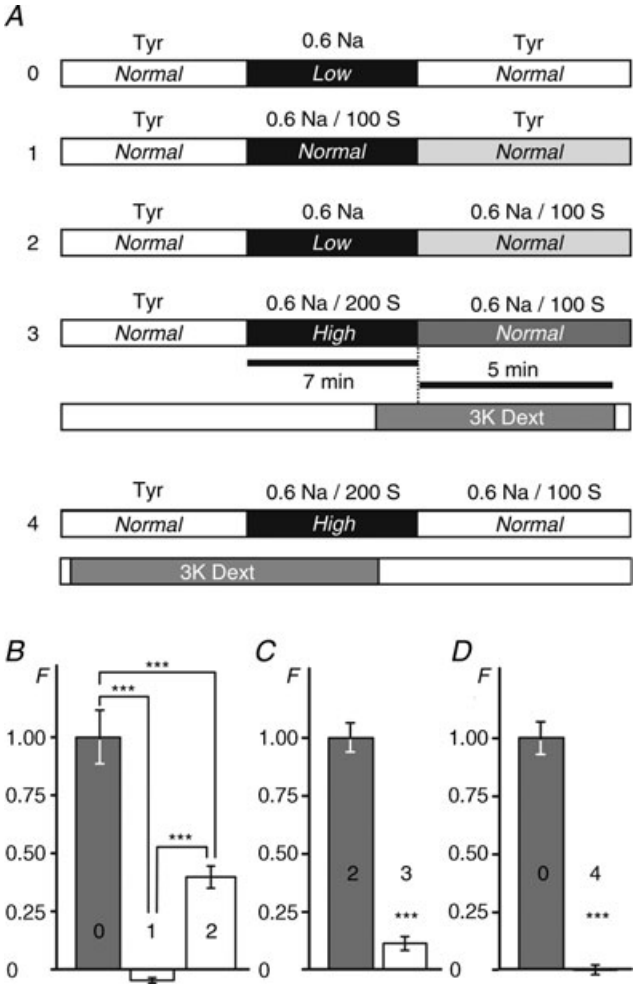

Figure 5. Effects of NaCl, osmolarity and cell shrinkage on t-tubular sealing
A, timing of the application of various modified solutions (protocols 0, 1, 2 and 3) using 'late' and 'early' application (protocol 4) of 3K fluorescent dextran. *B*, comparison of the outcomes of experiments using protocol 0 and protocol 1 shows that osmotic stress rather than a change in the concentration of NaCl is responsible for sealing of t-tubules. However, the extent of t-tubular sealing is modulated by the concentration of extracellular NaCl, as can be concluded by comparing the outcomes of experiments using protocol 0 and protocol 2. *C*, resolution of hyperosmotic stress equivalent to that produced by 100 mM sucrose (protocol 3) has little effect on t-tubular sealing. *D*, cell shrinkage early in response to the application of hyperosmotic solution (protocol 4) does not cause sealing of t-tubules as well. *F* is the relative fluorescence. Mean fluorescence for protocol 0 in *B* and *D* and protocol 2 in *C* was set to 1. Note that the small negative fluorescence in *B* reflects experimental error due to background correction.

However, and not contradictory to these findings, NaCl does play a significant role in regulating osmotically induced detubulation. Specifically, as shown in Fig. 5*B*, equal hyposmotic stress leads to different levels of detubulation at different concentrations of NaCl. When removal of hyposmotic stress occurs at a reduced concentration of NaCl (0.6 Na; protocol 2) the amount of trapped 3K dextran is reduced to 0.40 ± 0.05 ($n = 20$, 20 and 20 myocytes for background control, protocol 0 and protocol 2, respectively; $P < 0.001$) of that observed in the presence of a normal concentration of NaCl (protocol 0).

Given that in the above experiments the initial transition to test solutions proceeded from normal Tyrode solution, it is possible that some or all of the effects observed might be due to the effect of a reduction in NaCl rather than a decrease in osmolarity. However, no difference in the amount of trapped dextran ('late' application; as in Fig. 5; protocols 0–3) was observed whether cells were transitioned from Tyr (normal osmolarity, normal NaCl) to 0.6 Na or from 0.6 Na/100 S (normal osmolarity, low NaCl) to 0.6 Na (data not shown).

We also performed a 'reverse osmosis' experiment in order to test whether the resolution of hyperosmotic stress of a similar magnitude (equal to that provided by 100 mM sucrose) leads to a level of detubulation similar to that during hyposmotic challenge (Fig. 5*A*; protocols 2 *versus* 3). Importantly, in these experiments the concentration of NaCl was kept unchanged during the swelling and shrinkage phases. The data show that the effect is highly asymmetrical (Fig. 5*C*). Specifically, the amount of trapped dextran after hyperosmotic challenge with 0.6 Na/200 S solution (protocol 3) was only ~11% of that observed during hyposmotic challenge (protocol 2), i.e. 0.11 ± 0.03 *versus* 1.00 ± 0.06 ($n = 22$, 24 and 22 myocytes for background control, protocol 2 and protocol 3, respectively; $P < 0.001$).

Similar to the effects of NaCl in the initial control solution discussed above, virtually no dextran trapping was observed in experiments using hypertonic solutions (as in Fig. 5*A*, protocol 3) whether cells were transitioned from Tyr to Tyr/100 S or from 0.6 Na/100 S to 0.6 Na/200 S (data not shown).

One common feature of all the above experiments where dextran trapping was observed during 'late' application of dextran is the shrinking of the cells.

Therefore, it remains possible that a lack of significant dextran trapping upon washout of hyperosmotic 0.6 Na/200 S solution in the 'late' type of experiments (Fig. 5*C*) is because t-tubules were already sealed during the preceding swelling period and were no longer accessible to extracellular molecules. In order to test this hypothesis, we turned back to the 'early' type of experiment as in Fig. 2*A* (protocol 1) to check whether extracellular dextran is trapped upon application of 0.6 Na/200 S solution. The results were negative. No measurable trapping of extracellular dextran was observed after application of 0.6 Na/200 S hypertonic solution when compared with that produced by washout of 0.6 Na hypotonic solution (Fig. 5*D*), i.e. 1.00 ± 0.07 *versus* 0.00 ± 0.01 ($n = 15$; $P < 0.001$), for hypo- and hyperosmotic challenges, respectively.

Electrophysiological evidence of hyposmotic detubulation

There are at least three essentially independent but intrinsically linked electrophysiological measures of detubulation in ventricular myocytes, namely: (1) change in the membrane capacitance; (2) change in so-called I_{K1} tail currents at near resting membrane potential; and (3) change in I_{K1} 'inactivation' at hyperpolarized membrane potentials (Cheng *et al.* 2011).

In the first approach, membrane capacitance was measured in the whole-cell configuration of the patch-clamp technique using the built-in Clampex utility (see Methods). Ventricular myocytes were first treated with 0.6 Na hyposmotic solution, and C_M was then measured within ~2 h postshock in normal Tyr solution, concurrently with measurements of ionic currents. The data show (Fig. 6*D*) that hyposmotic shock leads to nearly 27% ($P < 0.01$) reduction in C_M, from 183.5 ± 19.5 ($n = 9$) to 134.5 ± 6.7 pF ($n = 14$) in control and treated myocytes, respectively, consistent with significant detubulation.

The second approach is based on a well-established experimental finding that large outward potassium currents flowing into the highly restricted t-tubular space lead to significant accumulation of local K^+. The latter, in turn, can be assessed electrophysiologically by measuring inward potassium currents flowing through t-tubular I_{K1} channels upon membrane repolarization to near the reversal potential corresponding to that at the normal extracellular concentration of K^+ (Yasui *et al.* 1993; Clark *et al.* 2001; Cheng *et al.* 2011). Figure 6 highlights the major features of the phenomena and the effects of detubulation

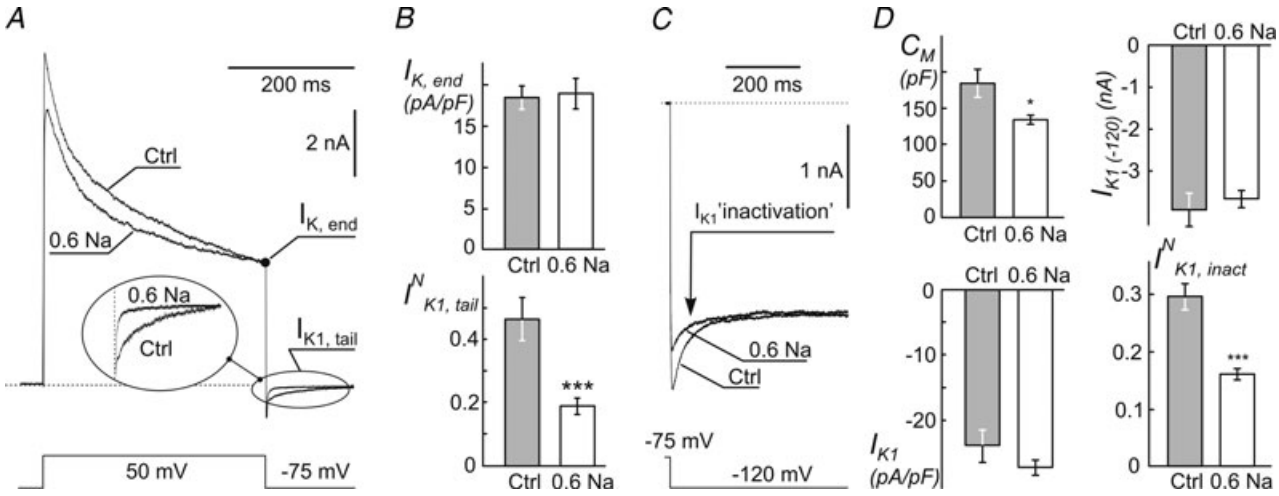

Figure 6. Electrophysiological evidence for sealing of t-tubules in response to resolution of hyposmotic stress
Myocytes were treated with 0.6 Na solution (as in Fig. 2) and whole-cell currents recorded with ~2 h postshock. *A*, representative current recordings in response to the indicated voltage step show a significant decrease in the amplitude of the I_{K1} tail current (inset) in. Individual myocytes with similar $I_{K,end}$ current were selected for presentation purposes. The amplitude of the I_{K1} tail current depends only on $I_{K,end}$, not the preceding part of the outward K^+ current (Cheng *et al.* 2011). The dotted horizontal line represents the zero current level. *B*, quantification of whole-cell $I_{K,end}$ and normalized I_{K1} tail currents ($I^N_{K1,tail}$; see Methods). *C*, inactivation of I_{K1} current at far negative membrane potentials (originates from depletion of t-tubular K^+ due to inward I_{K1} current) is significantly reduced in myocytes treated with 0.6 Na solution. The I_{K1} currents were recorded in response to a voltage step as indicated. Individual myocytes with similar steady-state values of I_{K1} current were selected for presentation purposes. *D*, quantification of changes in whole-cell membrane capacitance (C_M; top left panel), peak amplitude of whole-cell I_{K1} at −120 mV ($I_{K1(--120)}$; top right panel), density of peak I_{K1} (bottom left) and normalized inactivation of I_{K1} ($I^N_{K1,inact}$; bottom right; also see Methods).

induced by hyposmotic shock on various components of outward and inward K^+ currents, including so-called I_{K1} 'inactivation'. Experimentally, t-tubular accumulation of K^+ was induced by long-lasting outward K^+ currents in response to a voltage step from holding potential of −75 to +50 mV, which activates various voltage-dependent K^+ channels (Fig. 6*A*). Importantly, we have recently shown (Cheng *et al.* 2011) that the magnitude of t-tubular accumulation of K^+ depends essentially only on the magnitude of the K^+ current at the end of the voltage step (400 ms), and therefore, the relevant data are normalized to that current ($I_{K,end}$). With this in mind, for presentation purposes, Fig. 6*A* shows recordings from control and treated myocytes having values of $I_{K,end}$ of similar magnitude. Inspection of currents upon repolarization back to −75 mV shows that $I_{K1,tail}$ currents are significantly reduced in the myocyte treated with 0.6 Na hyposmotic solution (Fig. 6*A*, inset), suggesting significant detubulation. Interestingly, hyposmotic shock with 0.6 Na solution did not affect the density of $I_{K,end}$ itself (Fig. 6*B*, top panel), i.e. 18.5 ± 1.4 pA/pF ($n = 9$) and 19.0 ± 1.9 pA/pF ($n = 14$) in control and treated myocytes, respectively. Normalization of the amplitude of inward $I_{K1,tail}$ currents by $I_{K,end}$ (which underlies K^+ accumulation in t-tubules) takes care of cell-to-cell variation of this current, and the data provide an additional proof of significant detubulation ($I^N_{K1,tail}$; Fig. 6*B*, bottom panel). Specifically, the resolution of hyposmotic shock induced by 0.6 Na solution leads to a nearly 2.5-fold reduction of normalized $I_{K1,tail}$ current ($P < 0.001$) from 0.46 ± 0.07 ($n = 9$) to 0.19 ± 0.03 ($n = 14$).

The third electrophysiological approach is based on a similar phenomenon of restricted diffusion of K^+ in t-tubules. In ventricular myocytes, large inward I_{K1} currents flowing during membrane hyperpolarization beyond E_K reversal potential lead to depletion of t-tubular K^+, which can be observed as a time-dependent decline of I_{K1} current (called 'inactivation' in this case; Cheng *et al.* 2011). Figure 6*C* shows recordings of I_{K1} currents in selected control and treated myocytes chosen to have similar steady-state currents in order to highlight the effect of hyposmotic shock with 0.6 Na solution on I_{K1} 'inactivation'. The data clearly show a significant reduction in the amplitude of the time-dependent component of inward I_{K1} current ('inactivation') upon treatment of the myocytes with 0.6 Na solution. Quantified data presented in Fig. 6*D* (bottom right panel) point to significant detubulation as well. Specifically, the relative amplitude of I_{K1} 'inactivation' (normalized to the peak I_{K1} recalculated to time 0; $I_{K1(-120)}$) was reduced by approximately twofold ($P < 0.001$), from 0.30 ± 0.02 ($n = 8$) in control myocytes to 0.16 ± 0.01 ($n = 13$) in treated myocytes.

Surprisingly, despite significant loss of membrane capacitance (Fig. 6*D*) the peak amplitude of the whole-cell I_{K1} ($I_{K1(-120)}$; Fig. 6*D*) was essentially unaffected by hyposmotic shock, being -3.9 ± 0.4 ($n = 8$) and -3.7 ± 0.2 nA ($n = 13$) in control and treated myocytes, respectively. As a consequence of this, the density of I_{K1} was somewhat increased (however, not statistically significant; $P = 0.18$) after the treatment with hyposmotic 0.6 Na solution, suggesting potential upregulation of I_{K1} channels remaining in the outer sarcolemma after t-tubule sealing (this was not investigated further). Importantly, normalization of 'inactivating' currents takes care of changes in the activity of I_{K1} channels and strongly highlights a hidden stress-induced remodelling of the t-tubular system.

It may be argued that the changes in C_M and ionic currents are the result of slow recovery (recordings were performed within ∼2 h) of myocytes after the shock. Therefore, we have also performed experiments where ventricular myocytes were under the whole-cell voltage clamp during both application and removal of hyposmotic shock. Figure 7 shows an example of an experiment in which recordings of $I_{K1,tail}$ current (as in Fig. 6*A*) were taken immediately before the application hyposmotic solution, immediately before its removal and shortly after the resolution of the shock. For presentation purposes, the outward currents were normalized to each other at the end of the depolarization step. The example shows that normalized $I_{K1,tail}$ current is essentially not affected by the application of 0.6 Na hyposmotic solution but is significantly reduced shortly after its washout. Quantitatively, the average normalized $I_{K1,tail}$ currents before and during swelling were indistinguishable, 0.35 ± 0.04 *versus* 0.35 ± 0.04, respectively, but were reduced by more than fivefold to 0.064 ± 0.01 ($n = 10$; $P < 0.001$) right after the shock (Fig. 7, inset).

Changes in C_M measured during the same experiments were also consistent with sealing of t-tubules right upon resolution of hyposmotic stress. The average data were 157 ± 10, 156 ± 11 and 122 ± 6 pF ($n = 9$), before the application hyposmotic solution, before and after its removal, respectively. The data show a loss of ∼17% of C_M ($P < 0.001$) upon resolution of the hyposmotic shock.

Discussion

Numerous studies have investigated the effects of hyposmotic stress on various ion currents in ventricular cardiac myocytes. Besides Ca^{2+}, Cl^- and some K^+ currents mentioned in the Introduction, swelling significantly affects transient outward current (Wang *et al.* 2005), ATP-dependent K^+ current (Priebe & Beuckelmann, 1998) and Na^+ currents as well (Hu *et al.* 2009). Despite a wealth of data, the exact mechanisms underlying the observed effects remain to a large degree unknown. Two

obvious general mechanisms include a simple dilution of intracellular milieu and stretch of the membrane during the swelling phase. Both dilution and stretch, however, go away upon return to normal osmolarity. Less general mechanisms would involve activation of intracellular signalling systems leading, for example, to changes in channel phosphorylation (Missan *et al.* 2006, 2008).

In all previous studies, it was silently assumed that channels located in different membrane compartments of ventricular myocytes, including t-tubules and intercalated discs, respond to osmotic stress in a similar way. This is surely a very reasonable approximation, especially assuming a lack of approaches to separate the currents originating from different membrane compartments. However, even if one would suggest that ion channels respond in a similar manner to hyposmotic stress, there still exists another scenario of events in which those membrane compartments themselves may be affected. That, in turn, would lead to a hypothesis that at least some of the observed effects of hyposmotic stress may be explained by remodelling of t-tubules, which are known to harbour various ion channels and transporters (Brette & Orchard, 2007; Chase & Orchard, 2011). Dilatation or constriction of t-tubules may, for example, significantly affect the flow of ions through the t-tubular lumen, with predictable consequences on t-tubular membrane potential and ionic homeostasis. One of the well-studied phenomena in this area is t-tubular accumulation of K^+ due to the flow of outward K^+ currents through voltage-dependent K^+ channels (Clark *et al.* 2001). This effect is observed in normal freshly isolated ventricular myocytes and is a hallmark of intact t-tubules. One of the electrophysiological markers of t-tubular accumulation is a so-called I_{K1} tail current (Fig. 6; Yasui *et al.* 1993; Clark *et al.* 2001; Cheng *et al.* 2011). This current is not observed in ventricular myocytes detubulated using hyperosmotic shock with 1.5 M formamide (Cheng *et al.* 2011). Formamide-induced detubulation leads to significant changes in whole-cell ionic currents depending on the specific ion channel type. For example, it has been shown in an experiment employing formamide that about 80% of L-type Ca^{2+} channels reside in t-tubules (Brette *et al.* 2004). Clearly, osmotic stress of lesser degree (and different type, i.e. hyposmotic stress) may lead to varying degrees of t-tubular remodelling, probably including partial and/or even reversible constriction of the t-tubular lumen.

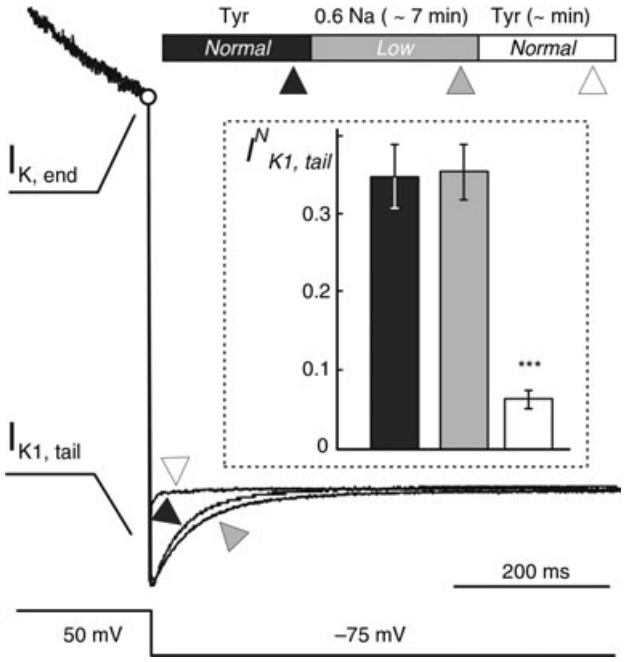

Figure 7. Time course of electrophysiological remodelling during hyposmotic stress
Example of whole-cell currents in response to a voltage protocol as in Fig. 6*A* recorded in the same myocyte at different times during hyposmotic stress and its resolution. Top bar shows the timing of the application of Tyrode solution (Tyr) and hyposmotic 0.6 Na solutions ('*Normal*' and '*Low*' osmolarity). Ionic currents were recorded within ~1–2 min before application of 0.6 Na solution (filled triangle), ~1–2 min before (shaded triangle) and ~3–6 min after its removal (open triangle). Current traces were normalized to each other at the end of the depolarizing voltage step ($I_{K,end}$; open circle) in order to highlight the relative changes in $I_{K1,tail}$ currents. The fast capacitative transient upon repolarization is not shown. Inset bar graph provides quantification of the data, showing that $I_{K1,tail}$ currents are not affected by the hyposmotic stress itself but are significantly reduced (by approximately fivefold; $P < 0.001$) shortly after resolution of the shock.

Unfortunately, to our knowledge, there is only one study in which the involvement of t-tubular remodelling in response to commonly used hyposmotic stresses was considered and tested. Specifically, Brette *et al.* (2000) used membrane labelling with di-8-ANEPPS to test whether hyposmotic swelling affects t-tubules in rat ventricular myocytes. The data showed that t-tubules remained accessible to the extracellular dye even after 10 min exposure to hyposmotic solution of ~180 mosmol (i.e. during the swelling phase) when myocytes displayed signs of truly severe stress (including membrane blebbing). The interpretation of the data is of importance, however. For example, if significant t-tubular constriction upon swelling did occur it still might not have been tight enough to prevent diffusion of relatively small di-8-ANEPPS dye through the constricted t-tubule lumen. In other words, the membrane labelling technique is useful only in detecting really tight constriction (although no number can be easily put here). In contrast, electrophysiological markers (e.g. I_{K1} tail currents; Clark *et al.* 2001; Cheng *et al.* 2011) of t-tubular integrity are useful in detecting even partial constriction or dilatation, although the quantitative interpretation of the data is fairly difficult at this time (Cheng *et al.* 2011). Therefore, the extent

and the direction of t-tubular remodelling (constriction or dilatation) during hyposmotic swelling remain an open question, although the results of the present study essentially rule out strong (or even measurable) sealing of t-tubules. Specifically, the data in Fig. 7 show that neither $I_{K1,tail}$ currents nor membrane capacitance is affected by swelling of the myocytes in any significant way.

In this regard, our recent findings show that 'hidden' t-tubular remodelling occurs even in conditions which are far from being as harsh as the exposure to 1.5 M formamide (Cheng *et al.* 2011). In particular, even simple dialysis of ventricular myocytes with commonly used intracellular solutions or poisoning with cyanide may lead to changes in various markers of t-tubular integrity or even to nearly complete detubulation. Therefore, in the present study we reassessed some consequences of hyposmotic swelling addressed by Brette *et al.* (2000) and went further by looking at the postshock state of t-tubules using different approaches.

The central, unexpected and equally important finding of our study is that the resolution of hyposmotic stress but not its induction leads to dramatic t-tubular remodelling (Fig. 2). In particular, washout of hyposmotic solution of $\sim$200 mosmol l^{-1} is associated with a loss of membrane capacitance (Fig. 6*D*, top left panel) comparable to that of the entire t-tubular system, trapping of extracellular dextran (Fig. 2) in sealed t-tubules and inaccessibility of a significant part of t-tubular system to di-8-ANEPPS dye applied after removal of the hyposmotic solution (Fig. 4).

The effects of short (a few minutes) exposure to hyposmotic solutions in several previous electrophysiological experiments (whole-cell patch clamp) are usually fully reversible (Li *et al.* 2002; Missan *et al.* 2011). This is seemingly inconsistent with our central finding that washout of 0.6 Na hyposmotic solution leads to nearly complete and nearly permanent detubulation (the fluorescence of trapped 3K dextran declines less than 10% h^{-1}; data not shown). Differences in species (mouse in this study *versus* guinea-pig, rat etc. in others) may be one of the underlying reasons. Experimental details may be of importance as well. In particular, the speed of washout of osmotic solutions may potentially contribute to the differences between the studies, with slower speeds leading to less abrupt and thus milder stress. The relevant quantitative data, however, are not available. Another plausible explanation is that the whole-cell dialysis (in whole-cell patch-clamp experiments) during cell swelling and shrinking may reduce the magnitude of stress with patch-pipette opening acting as a 'relief valve' against a build-up and resolution of intracellular pressure. Experiments with perforated patches (Missan *et al.* 2011) and the present experiments using the conventional whole-cell patch method (Fig. 7), however, are against this hypothesis. Nevertheless, it does not seem implausible that in many previous studies the t-tubules might have been lost even before application of the hyposmotic stress, either during the isolation procedure or soon after the establishment of the whole-cell configuration of the patch clamp. This hypothesis is strongly supported by our recent study showing that various types of relatively mild stress may lead to significant detubulation characterized, in particular, by the disappearance of electrophysiological markers of intact t-tubules, such as I_{K1} tail currents (Cheng *et al.* 2011). In further support for this, inspection of published whole-cell recordings of relevant K^+ currents shows that in several previous studies I_{K1} tail currents are essentially missing (London *et al.* 1998; Xu *et al.* 1999; Bodi *et al.* 2003; Borg *et al.* 2004; Wang *et al.* 2005), while they can be clearly seen in others (Tomita *et al.* 1994; Wickenden *et al.* 1999; Clark *et al.* 2001; Cheng *et al.* 2011), suggesting significant variability in the integrity of the t-tubular system due to different experimental conditions. The data in our study show that t-tubules are well preserved during the myocyte isolation procedure and various other manipulations (e.g. centrifugation steps) but can be easily sealed by the removal of hyposmotic stress.

Subcellular and molecular mechanisms of stress-induced sealing of t-tubules remain unclear. However, the strong regulatory effect of NaCl suggests the potential involvement of Na^+,K^+-ATPase and/or Cl^- channels. In this regard, the contribution of other major ions (e.g. K^+) and membrane transport systems (e.g. Na^+–Ca^{2+} exchanger) is also highly likely. However, addressing relevant underlying mechanisms is clearly beyond the scope of this study and will be investigated separately.

Physiological relevance

Swelling of cardiac myocytes is a common complication in various pathological conditions, including ischaemia (Vandenberg *et al.* 1996) or during application of cardioplegic solutions (Handy *et al.* 1996; Shaffer *et al.* 1998). Given that in most cases osmotic stress is resolved (or at least needs to be resolved), significant t-tubular remodelling may accompany the recovery from insult, leading to secondary complications. The described phenomenon formally resembles, and is likely to be linked to, a well-known effect of ischaemia–reperfusion injury (Kloner & Jennings, 2001), where the most severe complications occur not during the insult itself but during its resolution. The exact underlying mechanisms are likely to be different in every case, but it is also highly likely that t-tubular remodelling during reperfusion may be a significant contributor to an overall injury of the myocardium.

Conclusion

This study discloses a novel phenomenon of stress-induced t-tubular remodelling in ventricular myocytes. The data show that resolution but not induction of hyposmotic shock leads to a loss of membrane capacitance, changes in electrophysiological markers of t-tubular integrity and trapping of low-molecular-weight dextran inside the cells, all of which are consistent with the sealing of t-tubules.

References

Argiro V (1981). Excitation-contraction uncoupling of striated muscle fibres by formamide treatment: evidence of detubulation. *J Muscle Res Cell Motil* **2**, 283–294.

Bodi I, Muth JN, Hahn HS, Petrashevskaya NN, Rubio M, Koch SE, Varadi G & Schwartz A (2003). Electrical remodeling in hearts from a calcium-dependent mouse model of hypertrophy and failure: complex nature of K^+ current changes and action potential duration. *J Am Coll Cardiol* **41**, 1611–1622.

Borg JJ, Hancox JC, Hogg DS, James AF & Kozlowski RZ (2004). Actions of the anti-oestrogen agent clomiphene on outward K^+ currents in rat ventricular myocytes. *Clin Exp Pharmacol Physiol* **31**, 86–95.

Boyett MR, Frampton JE & Kirby MS (1991). The length, width and volume of isolated rat and ferret ventricular myocytes during twitch contractions and changes in osmotic strength. *Exp Physiol* **76**, 259–270.

Brette F, Calaghan SC, Lappin S, White E, Colyer J & Le Guennec JY (2000). Biphasic effects of hyposmotic challenge on excitation-contraction coupling in rat ventricular myocytes. *Am J Physiol Heart Circ Physiol* **279**, H1963–H1971.

Brette F, Komukai K & Orchard CH (2002). Validation of formamide as a detubulation agent in isolated rat cardiac cells. *Am J Physiol Heart Circ Physiol* **283**, H1720–H1728.

Brette F & Orchard C (2007). Resurgence of cardiac t-tubule research. *Physiology (Bethesda)* **22**, 167–173.

Brette F, Salle L & Orchard CH (2004). Differential modulation of L-type Ca^{2+} current by SR Ca^{2+} release at the T-tubules and surface membrane of rat ventricular myocytes. *Circ Res* **95**, e1–e7.

Cazorla O, Pascarel C, Brette F & Le Guennec JY (1999). Modulation of ions channels and membrane receptors activities by mechanical interventions in cardiomyocytes: possible mechanisms for mechanosensitivity. *Prog Biophys Mol Biol* **71**, 29–58.

Chase A & Orchard CH (2011). Ca efflux via the sarcolemmal Ca ATPase occurs only in the t-tubules of rat ventricular myocytes. *J Mol Cell Cardiol* **50**, 187–193.

Cheng L, Wang F & Lopatin AN (2011). Metabolic stress in isolated mouse ventricular myocytes leads to remodeling of t-tubules. *Am J Physiol Heart Circ Physiol* **301**, H1984–H1995.

Clark RB, Tremblay A, Melnyk P, Allen BG, Giles WR & Fiset C (2001). T-tubule localization of the inward-rectifier K^+ channel in mouse ventricular myocytes: a role in K^+ accumulation. *J Physiol* **537**, 979–992.

Eisenberg B & Eisenberg RS (1968). Selective disruption of the sarcotubular system in frog sartorius muscle. A quantitative study with exogenous peroxidase as a marker. *J Cell Biol* **39**, 451–467.

Groh WJ, Gibson KJ & Maylie JG (1996). Hypotonic-induced stretch counteracts the efficacy of the class III antiarrhythmic agent E-4031 in guinea pig myocytes. *Cardiovasc Res* **31**, 237–245.

Hamill OP, Marty A, Neher E, Sakmann B & Sigworth FJ (1981). Improved patch-clamp techniques for high-resolution current recording from cells and cell-free membrane patches. *Pflugers Arch* **391**, 85–100.

Handy JR Jr, Dorman BH, Cavallo MJ, Hinton RB, Roy RC, Crawford FA & Spinale FG (1996). Direct effects of oxygenated crystalloid or blood cardioplegia on isolated myocyte contractile function. *J Thorac Cardiovasc Surg* **112**, 1064–1072.

Howell JN (1969). A lesion of the transverse tubules of skeletal muscle. *J Physiol* **201**, 515–533.

Hu L, Ma J, Zhang P & Zheng J (2009). Extracellular hypotonicity induces disturbance of sodium currents in rat ventricular myocytes. *Physiol Res* **58**, 807–815.

Kawai M, Hussain M & Orchard CH (1999). Excitation-contraction coupling in rat ventricular myocytes after formamide-induced detubulation. *Am J Physiol Heart Circ Physiol* **277**, H603–H609.

Kloner RA & Jennings RB (2001). Consequences of brief ischemia: stunning, preconditioning, and their clinical implications: part 1. *Circulation* **104**, 2981–2989.

Li GR, Zhang M, Satin LS & Baumgarten CM (2002). Biphasic effects of cell volume on excitation-contraction coupling in rabbit ventricular myocytes. *Am J Physiol Heart Circ Physiol* **282**, H1270–H1277.

London B, Jeron A, Zhou J, Buckett P, Han X, Mitchell GF & Koren G (1998). Long QT and ventricular arrhythmias in transgenic mice expressing the N terminus and first transmembrane segment of a voltage-gated potassium channel. *Proc Natl Acad Sci U S A* **95**, 2926–2931.

Luo A-t, Luo H-y, Hu X-w, Gao L-l, Liang H-m, Tang M & Hescheler J (2010). Hyposmotic challenge modulates function of L-type calcium channel in rat ventricular myocytes through protein kinase C. *Acta Pharmacol Sin* **31**, 1438–1446.

McLerie M & Lopatin AN (2003). Dominant-negative suppression of I_{K1} in the mouse heart leads to altered cardiac excitability. *J Mol Cell Cardiol* **35**, 367–378.

Matsuda N, Hagiwara N, Shoda M, Kasanuki H & Hosoda S (1996). Enhancement of the L-type Ca^{2+} current by mechanical stimulation in single rabbit cardiac myocytes. *Circ Res* **78**, 650–659.

Missan S, Linsdell P & McDonald TF (2006). Role of kinases and G-proteins in the hyposmotic stimulation of cardiac I_{Ks}. *Biochim Biophys Acta* **1758**, 1641–1652.

Missan S, Linsdell P & McDonald TF (2008). Involvement of tyrosine kinase in the hyposmotic stimulation of I_{Ks} in guinea-pig ventricular myocytes. *Pflugers Arch* **456**, 489–500.

Missan S, Shuba LM, Zhabyeyev P & McDonald TF (2011). Osmotic modulation of slowly activating I_{Ks} in guinea-pig ventricular myocytes. *Cardiovasc Res* **91**, 429–436.

Priebe L & Beuckelmann DJ (1998). Cell swelling causes the action potential duration to shorten in guinea-pig ventricular myocytes by activating I_{KATP}. *Pflugers Arch* **436**, 894–898.

Rees SA, Vandenberg JI, Wright AR, Yoshida A & Powell T (1995). Cell swelling has differential effects on the rapid and slow components of delayed rectifier potassium current in guinea pig cardiac myocytes. *J Gen Physiol* **106**, 1151–1170.

Roos KP (1986). Length, width, and volume changes in osmotically stressed myocytes. *Am J Physiol Heart Circ Physiol* **251**, H1373–H1378.

Shaffer RF, Baumgarten CM & Damiano RJ Jr (1998). Prevention of cellular edema directly caused by hypothermic cardioplegia: studies in isolated human and rabbit atrial myocytes. *J Thorac Cardiovasc Surg* **115**, 1189–1195.

Soeller C & Cannell MB (1999). Examination of the transverse tubular system in living cardiac rat myocytes by 2-photon microscopy and digital image-processing techniques. *Circ Res* **84**, 266–275.

Sorota S (1992). Swelling-induced chloride-sensitive current in canine atrial cells revealed by whole-cell patch-clamp method. *Circ Res* **70**, 679–687.

Stewart JM & Page E (1978). Improved stereological techniques for studying myocardial cell growth: application to external sarcolemma, T system, and intercalated disks of rabbit and rat hearts. *J Ultrastruct Res* **65**, 119–134.

Tomita F, Bassett AL, Myerburg RJ & Kimura S (1994). Diminished transient outward currents in rat hypertrophied ventricular myocytes. *Circ Res* **75**, 296–303.

Vandenberg JI, Rees SA, Wright AR & Powell T (1996). Cell swelling and ion transport pathways in cardiac myocytes. *Cardiovasc Res* **32**, 85–97.

Vandenberg JI, Yoshida A, Kirk K & Powell T (1994). Swelling-activated and isoprenaline-activated chloride currents in guinea pig cardiac myocytes have distinct electrophysiology and pharmacology. *J Gen Physiol* **104**, 997–1017.

Wang GL, Wang GX, Yamamoto S, Ye L, Baxter H, Hume JR & Duan D (2005). Molecular mechanisms of regulation of fast-inactivating voltage-dependent transient outward K^+ current in mouse heart by cell volume changes. *J Physiol* **568**, 423–443.

Whalley DW, Hemsworth PD & Rasmussen HH (1991). Sodium–hydrogen exchange in guinea-pig ventricular muscle during exposure to hyperosmolar solutions. *J Physiol* **444**, 193–212.

Whalley DW, Hool LC, Ten Eick RE & Rasmussen HH (1993). Effect of osmotic swelling and shrinkage on Na^+-K^+ pump activity in mammalian cardiac myocytes. *Am J Physiol Cell Physiol* **265**, C1201–C1210.

Wickenden AD, Jegla TJ, Kaprielian R & Backx PH (1999). Regional contributions of Kv1.4, Kv4.2, and Kv4.3 to transient outward K^+ current in rat ventricle. *Am J Physiol Heart Circ Physiol* **276**, H1599–H1607.

Xu H, Guo W & Nerbonne JM (1999). Four kinetically distinct depolarization-activated K^+ currents in adult mouse ventricular myocytes. *J Gen Physiol* **113**, 661–678.

Yasui K, Anno T, Kamiya K, Boyett MR, Kodama I & Toyama J (1993). Contribution of potassium accumulation in narrow extracellular spaces to the genesis of nicorandil-induced large inward tail current in guinea-pig ventricular cells. *Pflugers Arch* **422**, 371–379.

Additional information

Competing interests

None declared.

Funding

This work was supported by R01-HL-069052 (A.N.L.) grant from the National Institutes of Health.

Author's present address

L. F. Cheng: 393 Xinyi Road, Department of Pharmacology, Xinjiang Medical University, Urumqi, Xinjiang 830001, China. Email: lewisclf@gmail.com